Proceedings of the Institute of Acoustics

RADIAL PRESSURE WAVES IN SLOTLESS-ROTOR INDUCTION MOTORS

Professor S. Williamson

University of Cambridge, Department of Engineering,
Trumpington Street, Cambridge. CB2 1PZ, U.K.

1. INTRODUCTION

Engineering design is inevitably a matter of compromise. The designer seeks to meet all of the specified performance objectives whilst at the same time attempting to keep other design quality indicators within acceptable limits. For an electrical motor the customer may specify supply voltage, frequency, speed, output power, starting torque, and shaft height, and many other things. A good design will not only meet the specification, but will also have a high efficiency, high power factor, small volume, acceptable noise level and, of course, low cost.

For cage induction motors most of the quality indicators are enhanced by choosing an air-gap length that is as small as possible, subject to considerations of the mechanical clearances attainable without recourse to expensive high-tolerance machining. The only quality indicator that is adversely affected by minimising the air-gap length is the acoustic noise. The problem here arises from the motion of the rotor teeth past the stator, resulting in a moving periodic disturbance in the air-gap field and, consequently, rotating radial pressure waves.

Certain steps are taken to minimise the acoustic effects of slotting. Slot openings are kept small, slot combinations known to be noisy are avoided, and the rotor is skewed. Although these steps may be successful in reducing the high-frequency noise due to slotting, they cannot eliminate it altogether. The high-frequency radial pressure waves can be eliminated, however, if the rotor is made slotless, that is, if the cage is replaced by a conducting sheet lying on the surface of a smooth laminated-iron rotor. Such an idea runs contrary to accepted design practice because it implies a large magnetic air-gap. In this respect it must be remembered that the air-gap is the distance between the iron surfaces, so that assuming the clearance betwen moving and stationary parts remains the same for slotted and slotless designs, the magnetic air-gap is increased by the thickness of the conducting sheet in the slotless machine.

This paper reports the preliminary results from an investigation into slotless-rotor induction motors. The purpose of the investigation is to quantify the possible benefits with respect to radial pressure wave production that might accrue from the use of slotless designs, whilst at the same time assessing the penalties to be paid in terms of the other performance indicators.

2. PRESSURE WAVE ANALYSIS

The effect that removing the rotor slots has on the modes and frequencies of the radial pressure waves may be understood by firstly considering the pressure waves produced in a conventional machine with a slotted rotor. It will be assumed in this respect that the machine is symmetrically constructed and is excited from a balanced three-phase supply. The method of force wave analysis used is based on the multiplication of permeance waves and mmf harmonics. This method has been chosen because it gives a clear indication of the origins of the component pressure waves whilst maintaining an acceptable accuracy for the calculation of the amplitudes of the predominant force-producing components. The method is described in detail by Yang [1].

The specific air gap permeance due to stator and rotor slotting may be written in the form:

$$\lambda(\theta,t) = \Lambda_0 \sum_{i=0}^{\infty} \sum_{j=0}^{\infty} a_i b_j \cos iN_S\theta \cos jN_R\left[\frac{\omega}{p}(1-s)t - \theta\right] \tag{1}$$

in which N_S and N_R are respectively the stator and rotor slot numbers, p is the pole-pair number for the fundamental flux wave, and s is the fractional slip. Λ_0 is the reciprocal of the effective air-gap length, and the harmonic permeance factors a_i and b_j depend on the stator and rotor slot geometry [2]. The resultant mmf waveform in a regular three-phase motor has the form:

$$F(\theta,t) = F_0 \sum_{k=-\infty}^{\infty} c_k \cos(\omega t - p(6k+1)\theta + \phi_k) \tag{2}$$

where F_0 is the amplitude of the fundamental mmf wave (i.e. $c_0 = 1$). Values of c_k and ϕ_k for $k \neq 0$ give the relative magnitudes and phase angles of the corresponding harmonic mmf waves. The air-gap flux density is obtained from

$$B(\theta,t) = \lambda(\theta,t)\, F(\theta,t)\mu_0 \tag{3}$$

and the radial pressure waves from

$$P(\theta,t) = \frac{1}{2\mu_0} B^2(\theta,t) \tag{4}$$

Substituting from equations 1 and 2 into 3 and 4 allows the pressure to be written in the form:

$$P(\theta,t) = P_0 \sum_{I=-\infty}^{\infty} \sum_{J=-\infty}^{\infty} \sum_{K=-\infty}^{\infty} \xi_{IJK}$$

$$\left[\cos\left[\left[2 + \frac{JN_R(1-s)}{p}\right]\omega t - \left[JN_R + IN_s + p(6K+2)\right]\theta + \phi_K\right]\right.$$

$$\left. + \cos\left[\frac{JN_R(1-s)}{p}\,\omega t - \left[JN_R + IN_s + 6pK\right]\theta + \chi_K\right]\right] \qquad (5)$$

In equation 5, J may be obtained from the sum of or difference between any two signed integers, corresponding to the interaction of the corresponding rotor slot permeance harmonics. This is also true for I and K which relate to the stator slot permeance and mmf harmonics respectively. ϕ_K and χ_K are phase angles derived from the appropriate values of ψ_k, and the amplitude ξ_{IJK} is obtained using the appropriate values of a_i, b_j and c_k. Finally P_0 is the magnitude of the fundamental pressure wave, given by:

$$P_0 = \frac{B_0^2}{4\mu_0} = \frac{\mu_0 \Lambda_0^2 F_0^2}{4} \qquad (6)$$

where B_0 is the peak fundamental flux density. Equation 5 is somewhat cumbersome for the determination of magnitudes, which are more readily accessed through consideration of individual interactions. It does however enable the rotor slotting to be identified as the cause of all components at frequencies other than twice supply frequency.

For a slotless rotor $N_R = 0$, so that equation 5 reduces to

$$P(\theta,t) = P_0 \sum_{I=-\infty}^{\infty} \sum_{K=-\infty}^{\infty} \zeta_{IK}\left[\cos\left[2\omega t - \left[IN_s + p(6K+2)\right]\theta + \phi_K\right]\right.$$

$$\left. + \cos\left[\left[IN_s + 6pK\right]\theta + \chi_K\right]\right] \qquad (7)$$

The second term in equation 7 is time-invariant and therefore does not contribute to radial vibration. The first term contains time-variation at twice supply frequency only, showing that all high-frequency radial force pulsations have been eliminated.

The term multiplying θ gives the mode number of the pressure wave. For a regular three-phase machine, i.e. one having an integral number of slots per pole and phase (= m) we may write

$$N_S = 6\ pm \tag{8}$$

therefore
$$IN_S + p(6K + 2) = 6p(mI + K) + 2p \tag{9}$$

Equation 9 shows that the lowest mode number in a slotless-rotor machine will be equal to the number of poles (i.e. 2p). All other mode numbers will be of the form $(3n \pm 1)2p$ which gives all multiples of the pole number which are not divisible by 3.

3. ELECTROMAGNETIC MODEL FOR SLOTLESS ROTOR MACHINES

The electromagnetic model used to investigate the performance of a slotless rotor machine is illustrated in Fig. 1, which shows a developed section through the machine, with both rotor and stator iron being represented by smooth laminated iron blocks [3]. The rotor conductor has radial thickness t, and clearance gap g. The stator excitation is modelled using a thin current sheet placed on the inside of the stator surface.

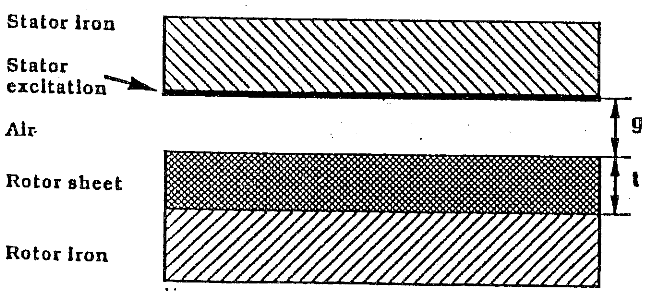

fig 1 Multilayer model for slotless-rotor machine

Whilst such a model gives a poor representation for the stator it gives a good representation for the rotor and air-gap as seen from the stator. The approach adopted, therefore, is to modify the standard equivalent circuit (shown in Fig. 2(a)) by replacing the air-gap and rotor sections by a combined impedance calculated using the layer model of Fig. 1. In fact the layer model allows the effects of stator harmonic mmfs to be taken directly into account, so that a more detailed equivalent circuit is used. This circuit, which is shown in Fig. 2(c), is essentially the same as the chain equivalent circuit used when harmonics are included in the standard equivalent circuit of Fig. 2(a). The component $\bar{Z}_{Rn}$ refers to the n^{th} harmonic stator mmf, and is calculated using the layer model as

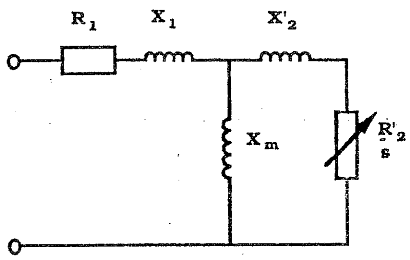

fig 2(a) Standard Equivalent Circuit

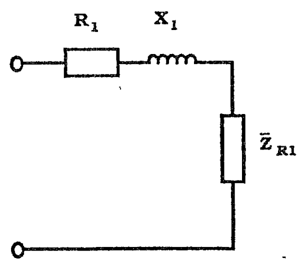

fig 2(b) Equivalent Circuit for slotless rotor, fundamental only

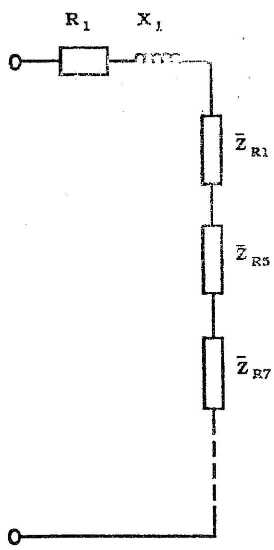

fig 2(c) Equivalent Circuit for slotless rotor, including harmonics

$$\bar{Z}_{Rn} = \frac{3j\mu_0 wf}{np} C_n^2 \left\{\frac{k + \gamma \tanh\gamma t \tanh kg}{k \tanh kg + \gamma \tanh\gamma t}\right\} \quad (10)$$

With $$\gamma = \left[k^2 + j2\pi f\mu_0\sigma s\right]^{\frac{1}{2}} \quad (11)$$

Where C_n = Effective conductors per phase for the n^{th} harmonic;
d = Mean diameter of air-gap;
f = Supply frequency;
k = Wave number = $\frac{2np}{d}$;
w = Stack length;
σ = Rotor conductivity.

The approach adopted, therefore, is to select a speed, calculate the impedances $\bar{Z}_{Rn}$ for the fundamental and most important harmonics, add in the stator resistance and leakage reactance, and finally calculate the input current, I. This then allows the input power, stator loss, and rotor input power to be determined directly from the equivalent circuit. The torque developed is determined by summing harmonic components.

$$T = \frac{3pI^2}{2\pi f} \Sigma\, n\, R_e[\bar{Z}_{Rn}] \quad (12)$$

The amplitude of the n^{th} harmonic flux density is determined from

$$B_n = \frac{kI}{\sqrt{2}\pi f w C_n} |\bar{Z}_{Rn}| \quad (13)$$

4. INITIAL DESIGN STUDY

A design study has now been carried out, based on a particular industrially-manufactured motor. The principal design and performance features of this machine are listed in Table 1, below.

Supply voltage	254 V (phase)
Supply frequency (f)	60 Hz
Pole number (2p)	6
Air-gap length (g)	1.0 mm
Mean air-gap diameter (d)	217 mm
Stack length (w)	197 mm
Outside diameter	317.5 mm
Rated efficiency	89.3 %
Rated power factor	0.79
Rated output power	15 kW
Rated current	27.9 A

Table 1. Details of Original Slotted Machine

The objective of the study was to design a slotless-rotor machine developing the same rated output power, and to compare the performance of the two. The principle variables in the design are the mean air-gap diameter and the thickness of the rotor conducting sheet.

As a basis for an initial design study it was decided to keep the flux per pole equal to that used in the original slotted machine. This was done to enable the same back-iron thickness and stator tooth width to be used in the new design. The increase in the electromagnetic air-gap from g to g+t to accommodate the rotor conductor implies that the magnetising current will be the dominant component in the input current at low slip (i.e. at the operating speed). For a fixed flux per pole, the magnetising ampere-turns vary in proportion with (g+t)/d, showing that the conducting sheet should be made as thin as possible and the stator diameter increased as far as practicable. Increasing the stator diameter also increases the area available for copper, since the tooth dimensions have been kept constant. As the stator diameter is increased, therefore, the stator resistance falls and the increased joule losses which are incurred by the stator windings because of the increase in the magnetising current are brought under control.

For this preliminary study, a value of conductor sheet thickness of t = 6.0 mm was selected and the diameter was progressively increased until a stator joule loss approximately equal to that of the slotted machine was achieved. This lead to the choice d = 290 mm, giving an overall diameter of 392.5 mm, which is 24% greater than the original. It was also noted that the rotor conducting sheet would need to be slit in a manner which simulated skewing by one stator slot pitch, other- wise unacceptably high losses would be produced by the stator slot harmonic fields. Table 2 gives a comparison between the calculated performance for the two machines.

	Starting		Full-load		
	Current	Torque	Current	Efficiency	Input VARS
Slotted Rotor	153.2	214	27.9	89.3%	13.0 kVAR
Sheet Rotor	300.4	420	35.0	87.0%	20.3 kVAR

Table 2. Performance Comparison

5. CONCLUSIONS

The use of a sheet rotor in an induction motor eliminates the high-frequency radial force pulsations caused by the rotor teeth. The remaining radial force waves all vary at twice supply frequency with a minimum mode number equal to the number of poles of the exciting wave. A slotless rotor machine will have a larger magnetic air-gap which therefore requires more ampere-turns to magnetise. As a consequence, the input VAR requirement will be increased, as will the overall envelope of the machine. It is, nevertheless, believed that there are applications where these penalties will be justified in terms of the reduction in electromagnetically-excited acoustic noise.

6. REFERENCES

[1] S J YANG, 'Low-noise electrical motors', Clarendon Press, Oxford (1981).
[2] B HELLER & V HAMATA, 'Harmonic effects in induction machines', Elsevier Scientific Publishing Co., Amsterdam (1977).
[3] E M FREEMAN, 'Travelling waves in induction machines: input impedance and equivalent circuits', Proc.IEE, Vol.115, No.12, pp.1772-1776 December (1968).